

SI Appendix

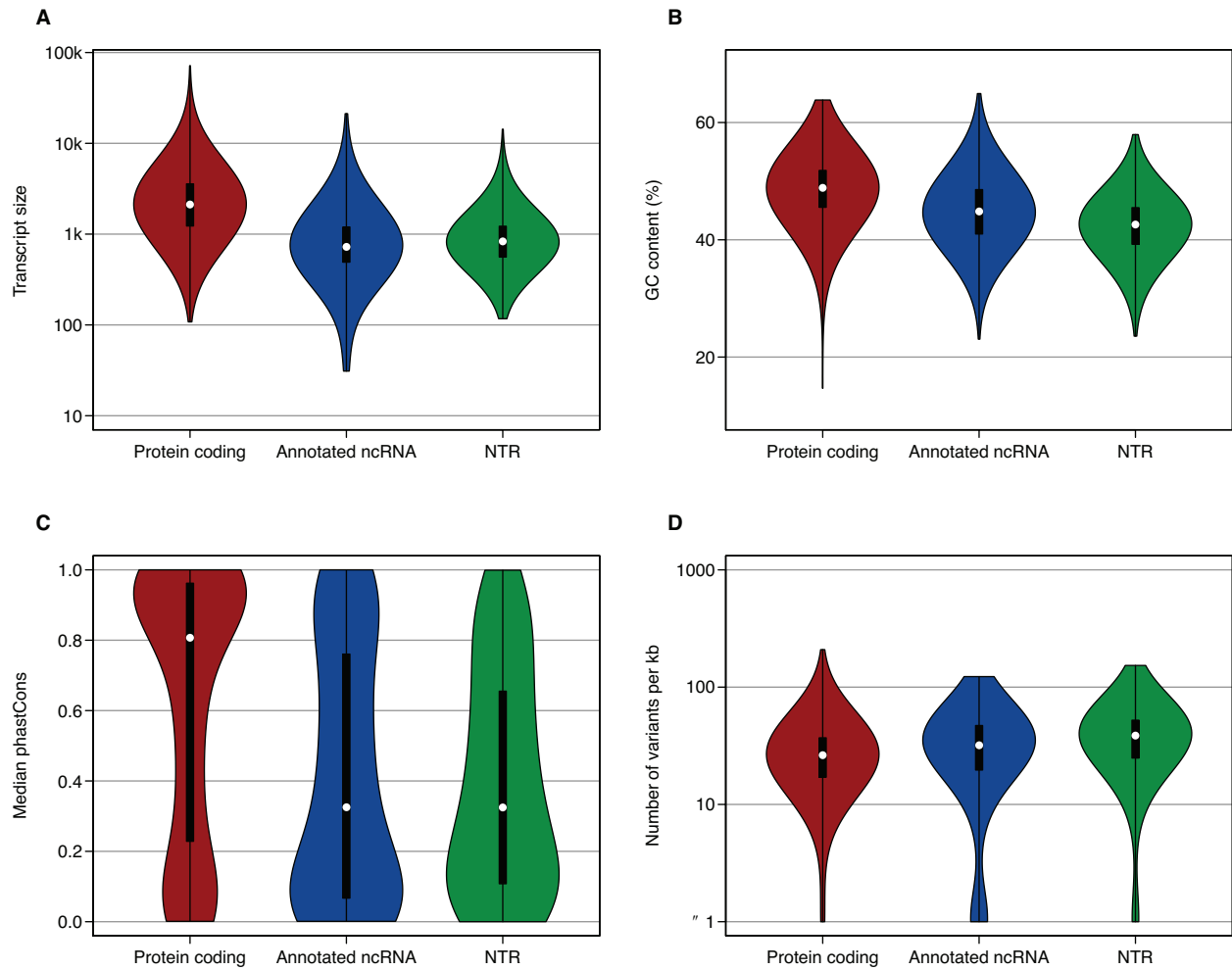


Figure S1. Genomic characteristics of annotated genes and NTRs. Violin plots showing (A) the distribution of transcript size, (B) GC content, (C) sequence conservation, and (D) variant density for annotated protein-coding genes, ncRNAs, and NTRs.

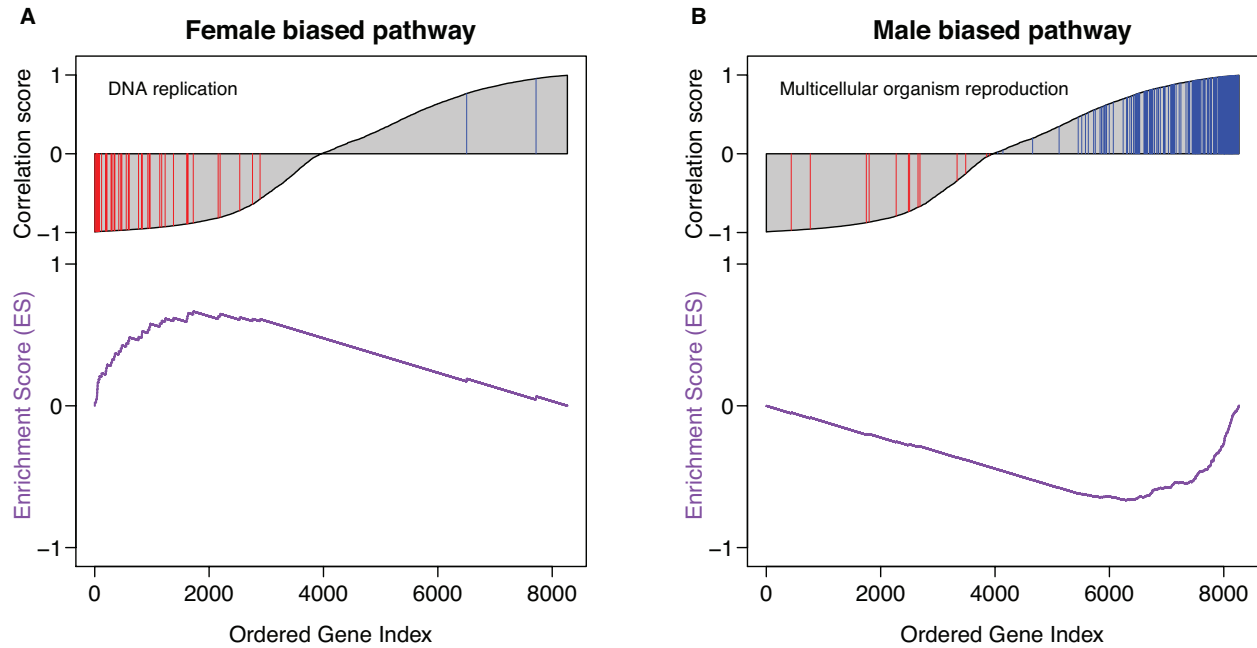


Figure S2. Gene sets enriched for female- and male-biased transcripts Examples of significant gene sets enriched for (A) female-biased and (B) male-biased transcripts, from gene set enrichment analysis performed on genes ranked according to their sexual dimorphism in expression. The sexual dimorphism is measured by the correlation score, which is calculated as $s(t)\sqrt{\frac{t^2}{n-2+t^2}}$, where n is the number of lines and $s(t)$ indicates the sign of the t statistic for the difference in expression between males and females. Red and blue vertical bars indicate respectively the positions of female-biased and male-biased transcripts among the tested pathways on the ranked list. The purple line indicates the running enrichment score in the gene set enrichment analysis.

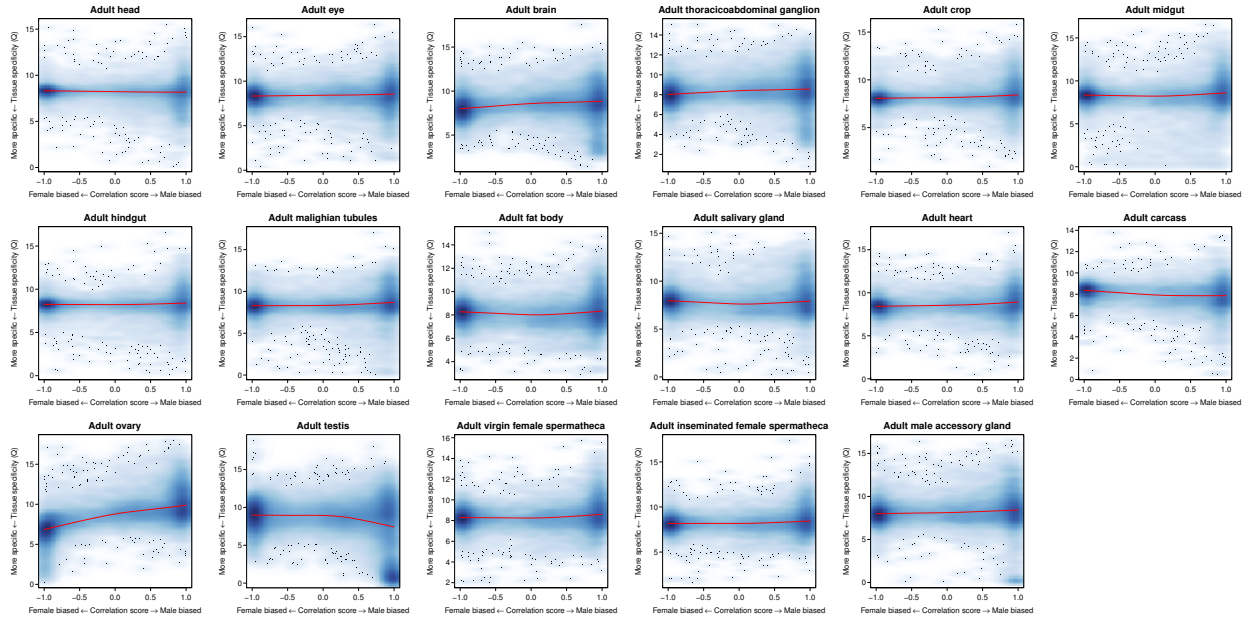


Figure S3. Tissue-specific expression of sexually biased transcripts. Tissue specificity of transcripts was calculated using the FlyAtlas gene expression profiles of 17 adult tissues as $Q_{g|t} = -\log_2(p_{t|g}) + \sum_{t=1,2,\dots,N} -p_{t|g} \log_2(p_{t|g})$, where $p_{t|g} = e_{g,t}/(e_{g,1} + e_{g,2} + \dots + e_{g,N})$ is the weighted expression of gene g in tissue t . $Q_{g|t}$ is smaller when expression of gene g is more specific in tissue t . In each tissue indicated, $Q_{g|t}$ for all genes is plotted against the extent of sexual dimorphism as measured by the correlation score. The density of points on the plots is indicated by darkness of the color. The red line represents a smoothed curve computed by LOESS regression fit.

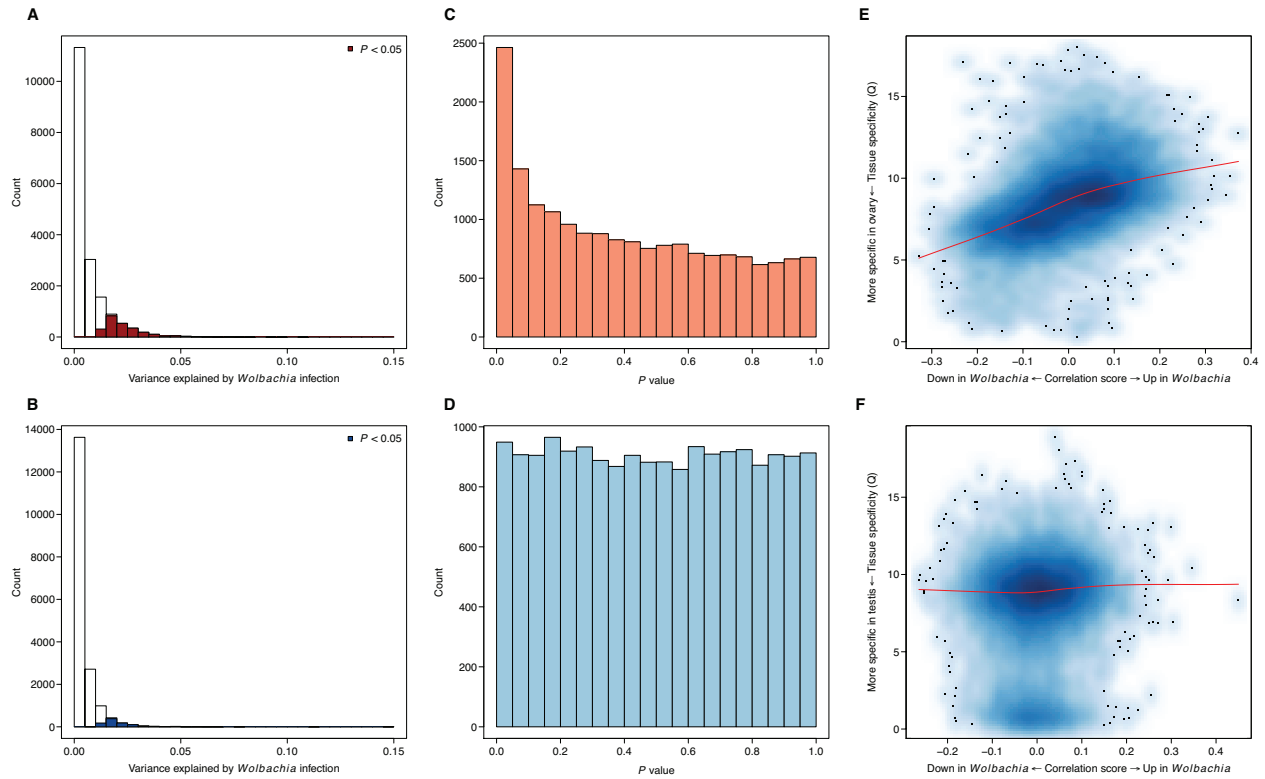


Figure S4. Effects of *Wolbachia* infection on gene expression The effect of *Wolbachia* infection on gene expression was tested using a linear mixed model accounting for inversions and main PCs of the genotype matrix. The variance in gene expression explained by the presence or absence of *Wolbachia* is estimated as $p(1 - p)w^2$, where p is the proportion of lines infected by *Wolbachia* and w is the estimated mean change in gene expression upon infection. (A and B) Histograms of variance explained by *Wolbachia* infection. Colors indicate nominally significant transcripts. (A) Females. (B) Males. (C and D) Distributions of P-values for the *Wolbachia* effects, indicating a female-specific effect of *Wolbachia*. (C) Females. (D) Males. (E and F) Reproductive tissue specificity of transcripts with respect to their *Wolbachia* effect. (E) Specificity of ovary expression for genes expressed in females. (F) Specificity of testis expression for genes expressed in males. Genes that are down-regulated in *Wolbachia*-infected females show ovary-specific expression.

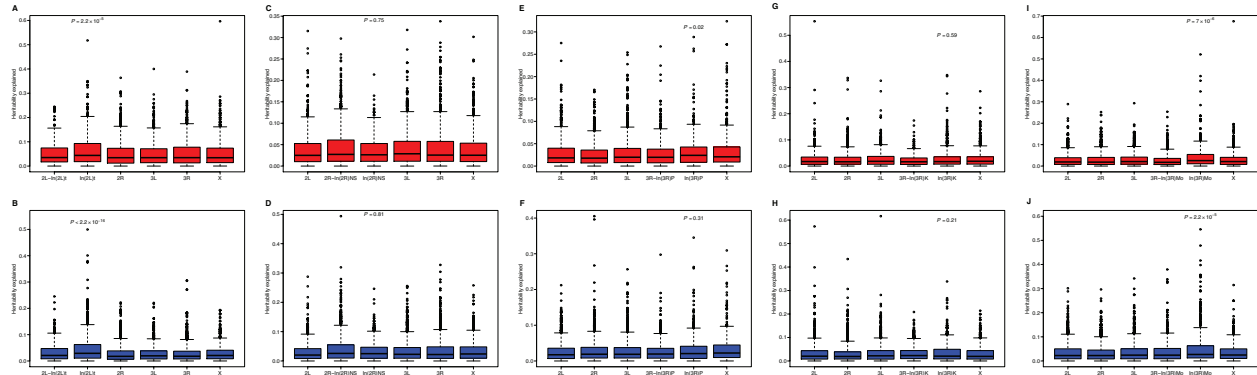


Figure S5. Effects of inversions on gene expression. The effects of major inversions on gene expression were tested using a linear mixed model accounting for inversions and main PCs of the genotype matrix. The variance explained by each inversion was estimated as $p_0v_0^2 + p_1v_1^2 + p_2v_2^2$, where p_i ($i = 0, 1, 2$) are the frequencies of lines that carry 0, 1, or 2 copies of the inverted karyotypes, and v_i ($i = 0, 1, 2$) are the estimated effects of each karyotype. This variance was divided by the total genetic variance to obtain the heritability explained by the inversions. (A–J) Plots depicting the heritability explained for transcripts, grouped according to their chromosomal regions for each of five major inversions. To test whether inverted regions are enriched for expression of genes affected by the inversion, the heritability of gene expression explained for genes in that region was compared with the remaining of the genome by a Wilcoxon test. The P -values from this test are indicated on each plot. (A) *In(2L)t*, females. (B) *In(2L)t*, males. (C) *In(2R)NS*, females. (D) *In(2R)NS*, males. (E) *In(3R)P*, females. (F) *In(3R)P*, males. (G) *In(3R)K*, females. (H) *In(3R)K*, males. (I) *In(3R)Mo*, females. (J) *In(3R)Mo*, males.



Figure S6. Examples of enrichment of biological pathways in MMC modules. The top three panels (red font) are for genetically correlated transcriptional modules in females, and the bottom four panels (blue font) are for male transcriptional modules. In each panel, the color of the text (GO name) represents different levels of FDR according to the scale bar on the right. The size of the text represents the factor of enrichment with the scale for no enrichment (factor =1) indicated in the top left corner of each panel.

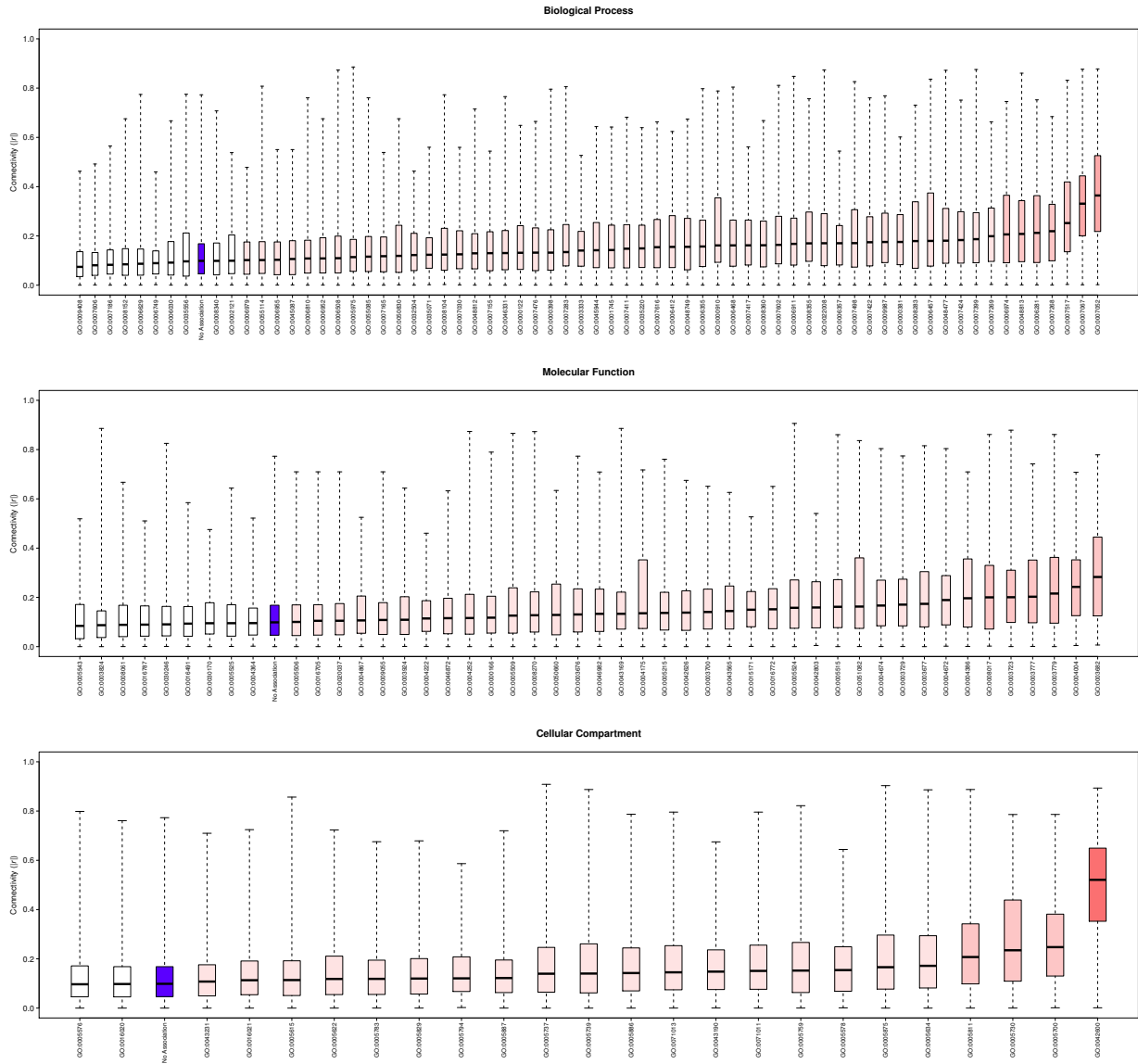


Figure S7. Genes within the same biological pathways have highly correlated expression in females. The box plots show the average connectivity (absolute correlation coefficient) within each GO pathway. The blue box depicts the connectivity among genes that have no known GO association.

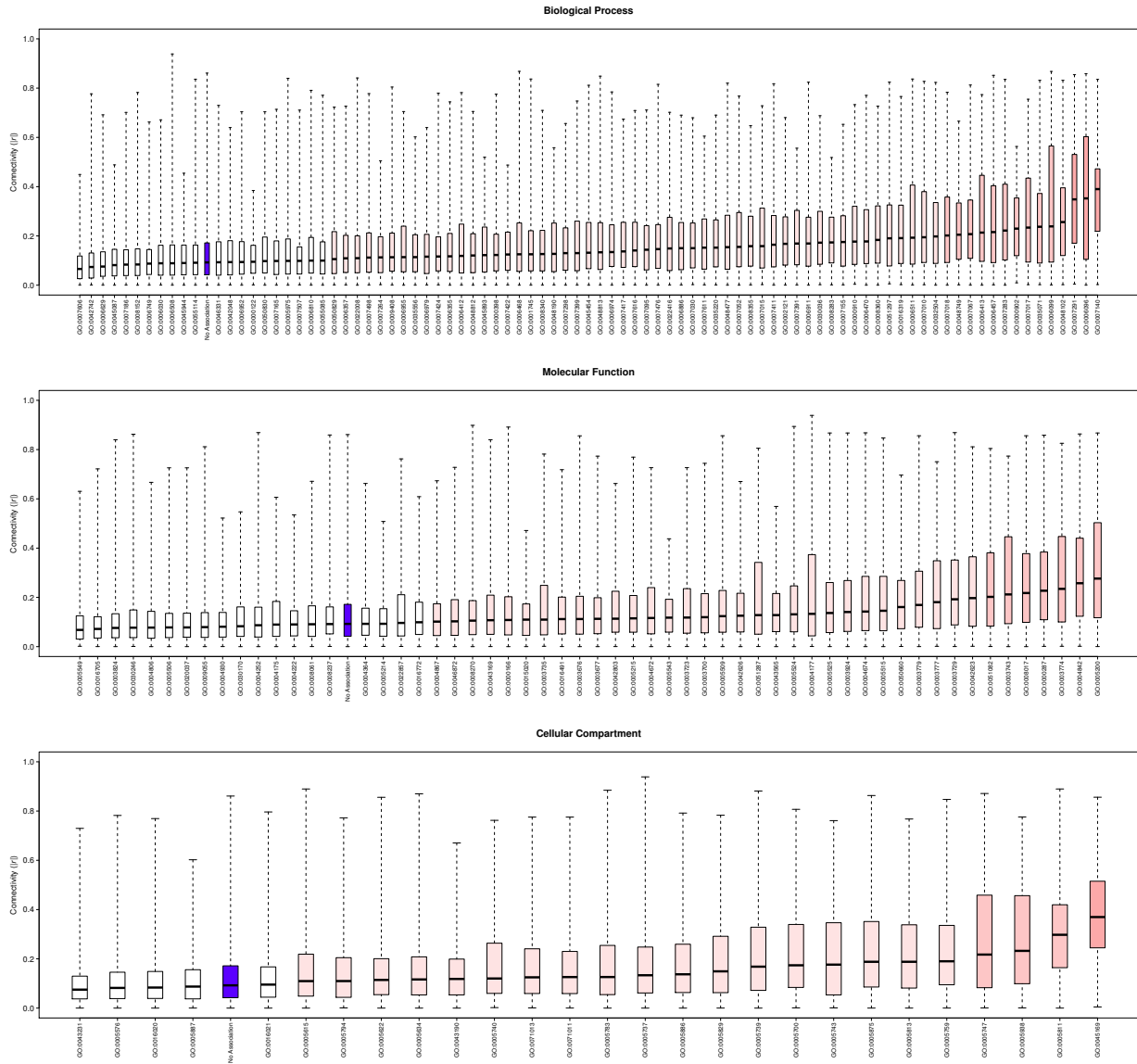


Figure S8. Genes within the same biological pathways have highly correlated expression in males. The box plots show the average connectivity (absolute correlation coefficient) within each GO pathway. The blue box depicts the connectivity among genes that have no known GO association.

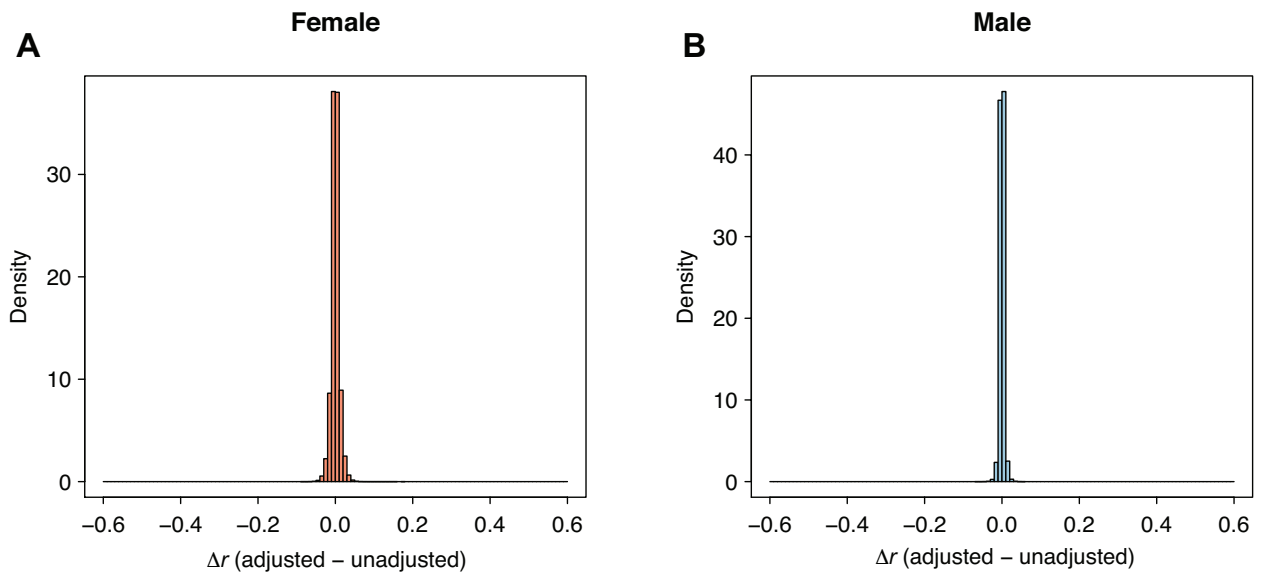


Figure S9. *Wolbachia* infection has a minimal effect on genetic correlation of gene expression. (A and B) Distributions of the difference between correlation coefficients between all pairs of genetically variable transcripts calculated with or without adjusting for the effect of *Wolbachia* infection on gene expression. (A) Females. (B) Males.

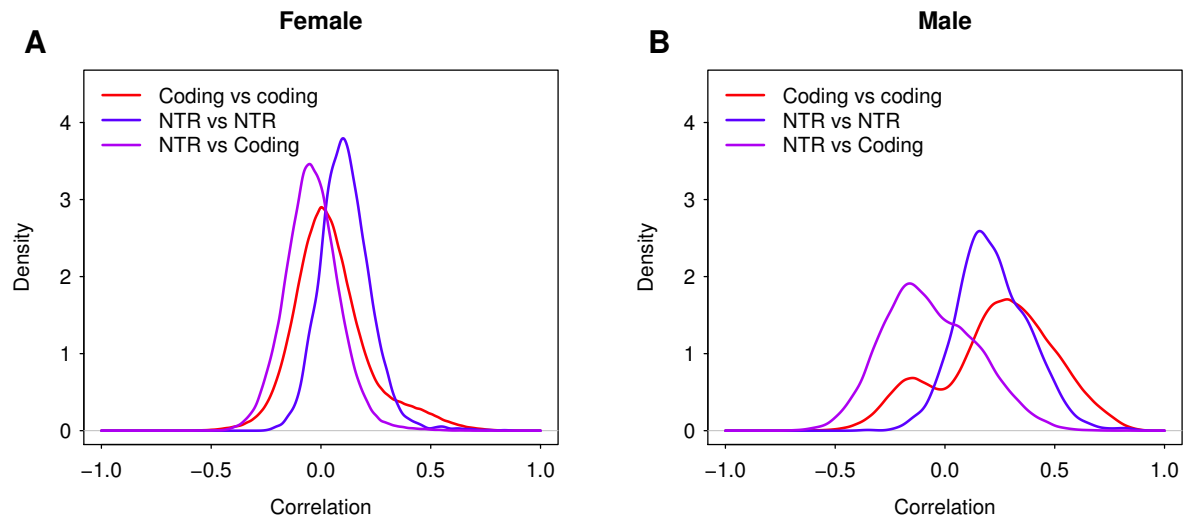


Figure S10. NTRs are negative regulators. (A and B) Distributions of correlation coefficients between protein-coding genes, between NTRs, and between NTRs and protein-coding genes, all within the same modules. (A) Females. (B) Males.

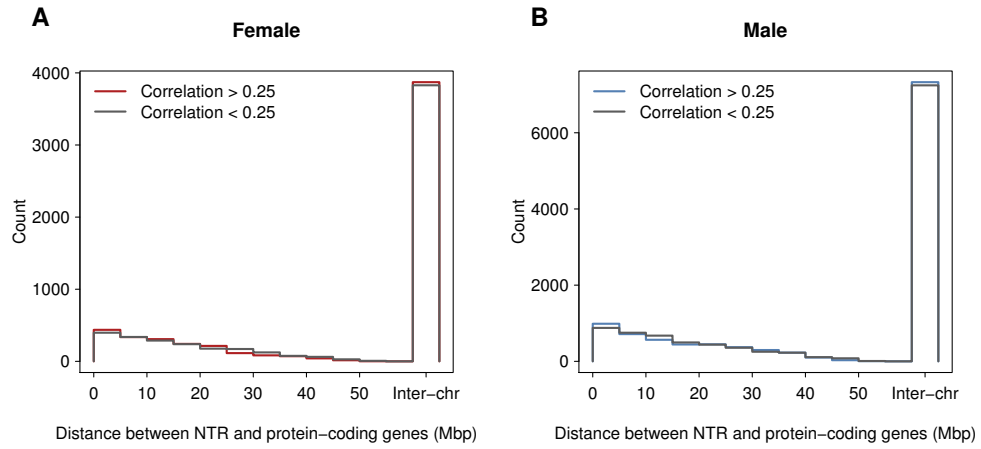


Figure S11. Distance between NTRs and protein coding genes. Distance between NTRs and protein-coding genes whose genetic correlation is greater than 0.25 within the same module or less than 0.25 in females (A) and males (B).

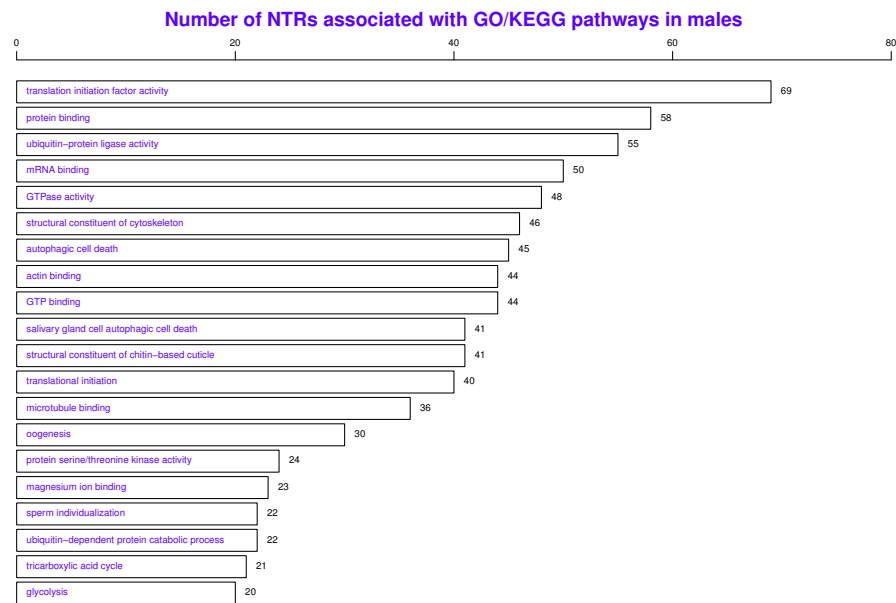
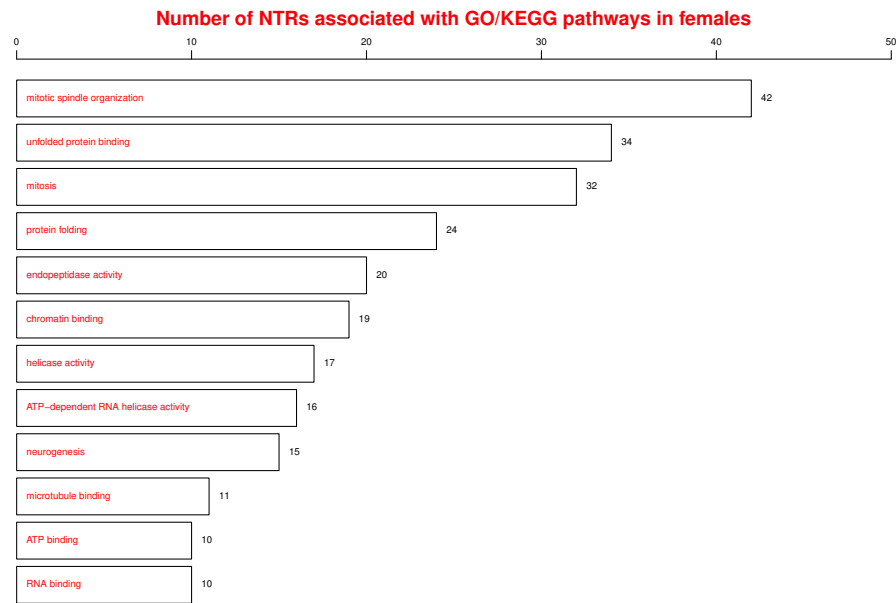


Figure S12. Functional annotation of NTRs. Annotation by association of NTRs with GO/KEGG pathways. The numbers of NTRs associated with GO/KEGG pathways are plotted for females (top panel) and males (bottom panel).

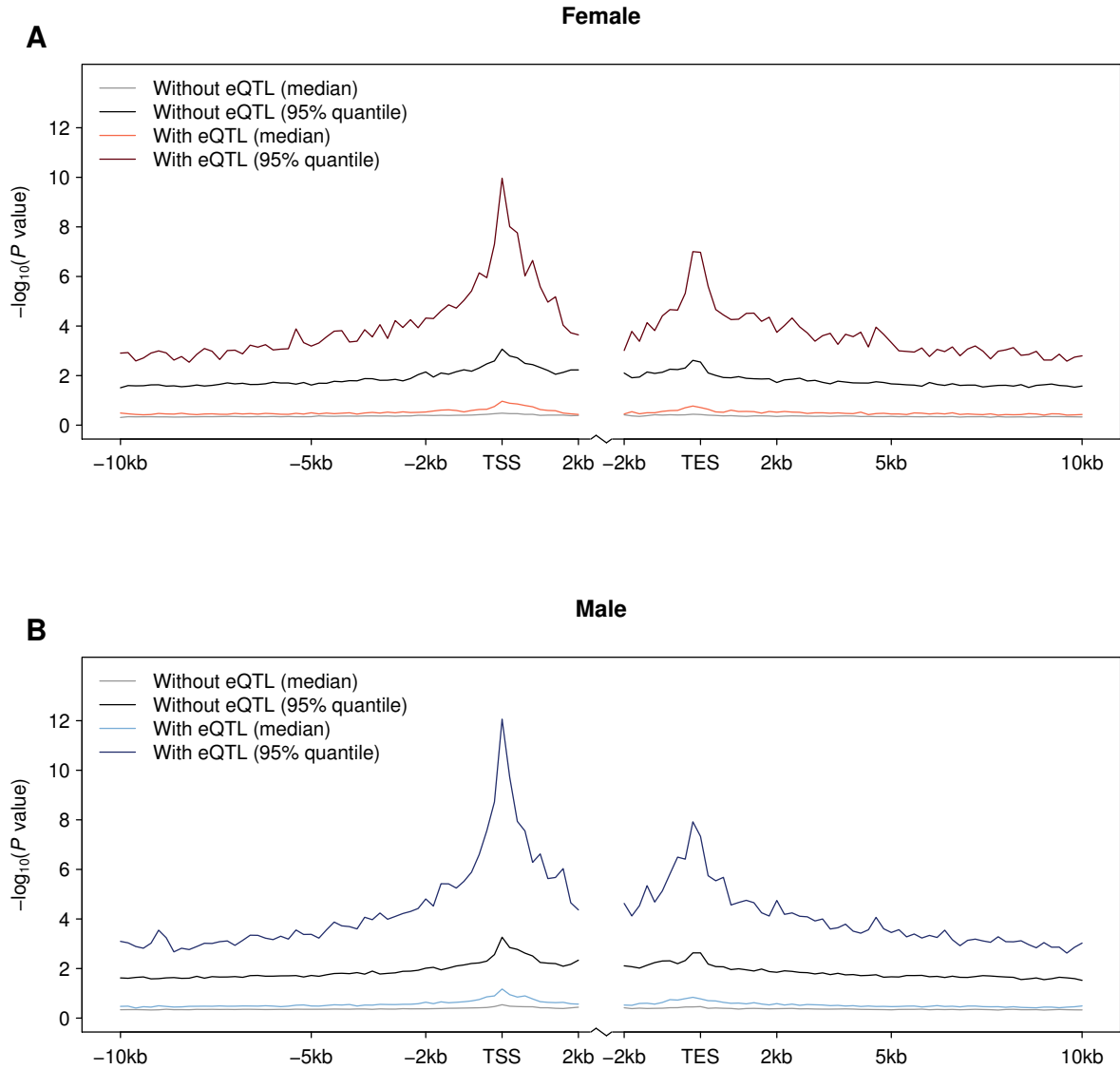


Figure S13. Strength of association between local variants and gene expression. (A and B) The plots depict the strength of association ($-\log_{10}P$) between DNA variants and gene expression (y-axis) against the distance relative to transcription start sites (TSS) or transcription end sites (TES). The figures show both the 95% quantile and median of $-\log_{10}P$ for variants within each non-overlapping 200bp window, plotted against the midpoint of the window. Negative and positive distances indicate, respectively, positions upstream and downstream of the direction of transcription. The analysis is shown for gene expression traits with (FDR < 0.20) and without (FDR \geq 0.2) eQTL. (A) Females. (B) Males.

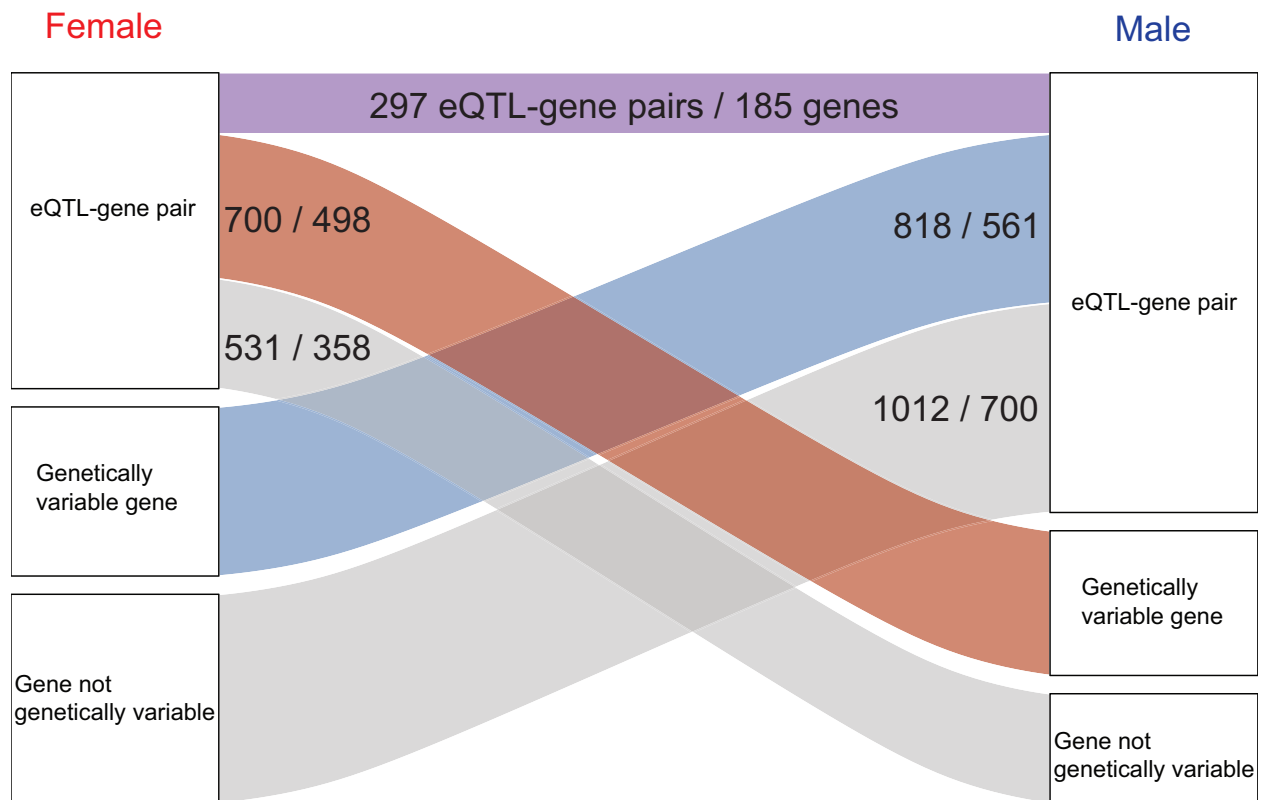


Figure S14. Sex-specific eQTLs Boxes on the left and right indicate the numbers of eQTL-gene pairs in females and males respectively. Ribbons (with the corresponding numbers of eQTL-gene pairs or genes) connect portions of the boxes that share the same eQTL-gene pairs or genes. The purple ribbon indicates shared eQTL-gene pairs in both sexes. The light red ribbon indicates eQTL-gene pairs that are significant only in females but not in males where the genes are also genetically variable. The light blue ribbon indicates eQTL-gene pairs that are significant only in males but not in females where the genes are also genetically variable. Grey ribbons indicate eQTL-gene pairs significant in one sex but not the other where the genes are not genetically variable.

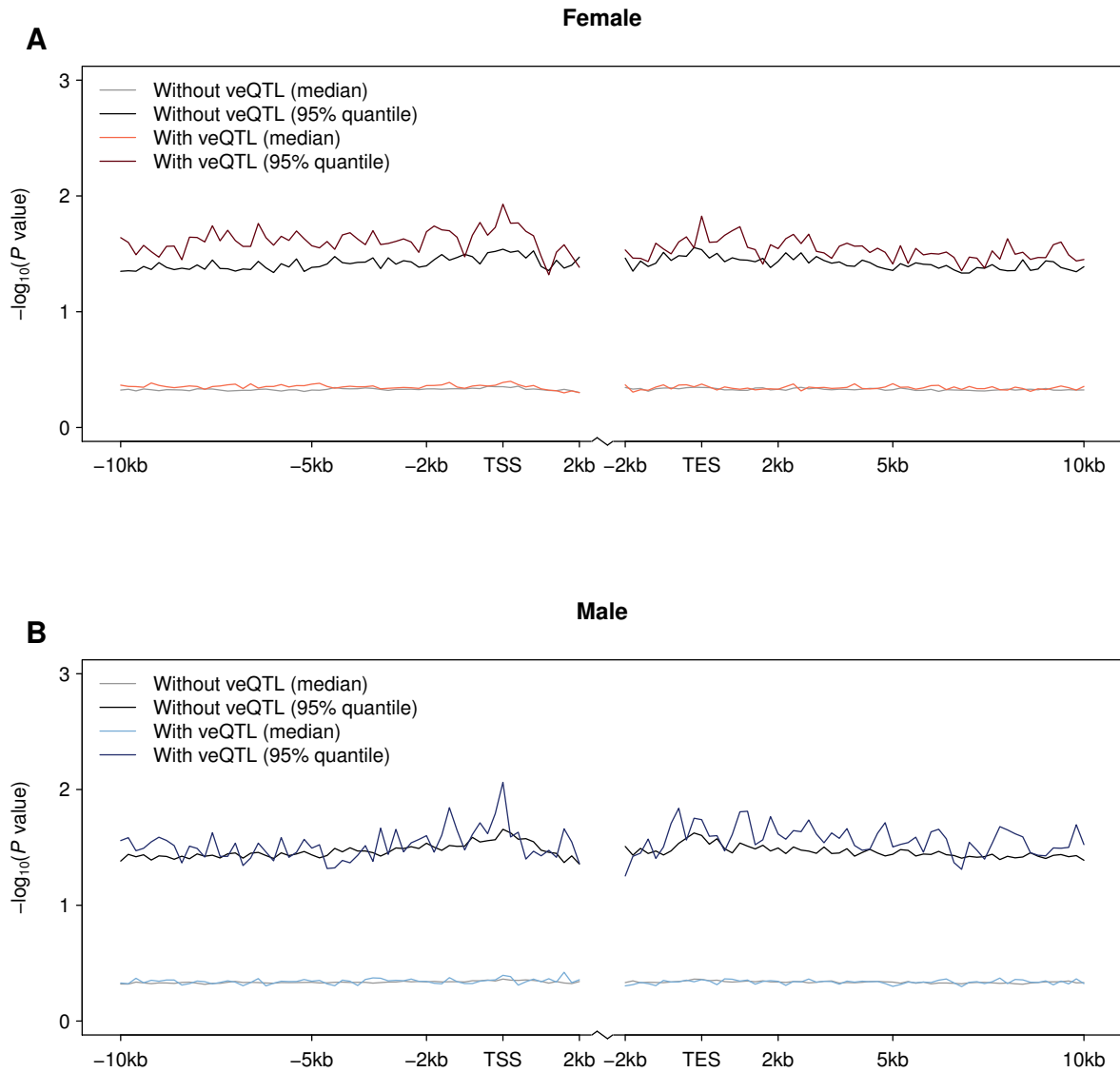


Figure S15. Strength of association between local variants and variance of gene expression. (A and B) The plots depict the strength of association ($-\log_{10}P$) between DNA variants and variance of gene expression (y-axis) against the distance relative to transcription start sites (TSS) or transcription end sites (TES). The figures show both the 95% quantile and median of $-\log_{10}P$ for variants within each non-overlapping 200bp window, plotted against the midpoint of the window. Negative and positive distances indicate, respectively, positions upstream and downstream of the direction of transcription. The analysis is shown for gene expression traits with (FDR < 0.20) and without (FDR \geq 0.2) veQTL. (A) Females. (B) Males.

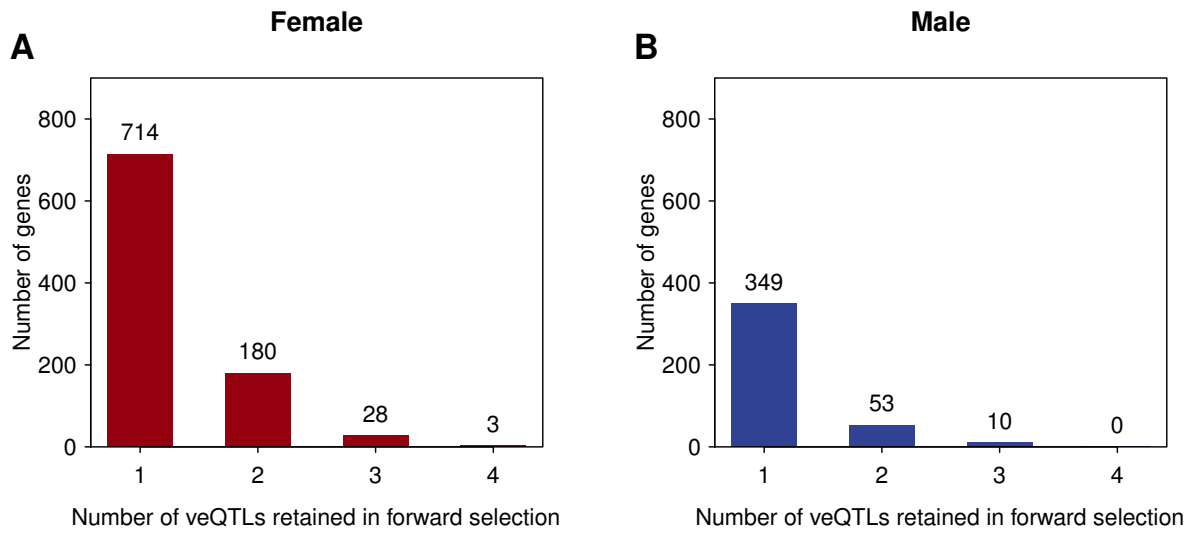


Figure S16. veQTLs retained in model selection. (A and B) Distributions of the numbers of veQTLs retained in forward model selection. (A) Females. (B) Males.

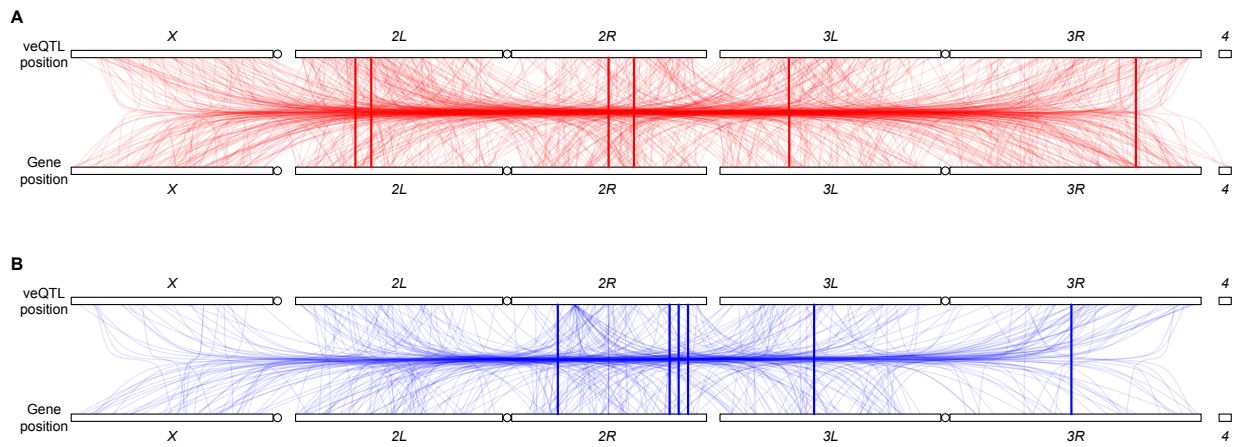


Figure S17. veQTLs are involved in epistatic interactions with *cis* variants. (A and B) Epistatic interactions between veQTLs and *cis* variants. (A) Females. (B) Males. Each veQTL and *cis* variant pair is connected by a light line. Interactions between *cis* veQTL and *cis* variants are highlighted by dark lines.